PERFORMANCE OF CONVOLUTIONALLY ENCODED NONCOHERENT MFSK MODEM IN FADING CHANNELS[1]

J. W. MODESTINO and S. Y. MUI
R.P.I.
Troy, N.Y.

Summary. The performance of a convolutionally encoded noncoherent multiple frequency shift-keyed (MFSK) modem utilizing Viterbi maximum likelihood decoding and operating on a fading channel is described. Both the lognormal and classical Rician fading channels are considered for both slow and time-varying channel conditions. Primary interest is in the resulting bit error rate as a function of E_b/N_0 parameterized by both the fading channel and code parameters. Fairly general upper bounds on bit error probability are provided and compared with simulation results in the two extremes of zero and infinite channel memory. The efficacy of simple block interleaving in combatting channel memory effects are thoroughly explored. Both quantized and unquantized receiver outputs are considered.

Introduction. Considerable attention has been focused recently [1]-[3] on the use of efficient error control coding in conjunction with noncoherent signaling on fading channels. Here the transmitted signal is known to undergo fading as a result of some appropriately defined channel scattering mechanism. As a result, coherent signaling schemes are either completely inappropriate or grossly inefficient. In this paper we describe the implementation and performance of a noncoherent multiple frequency-shift keyed (MFSK) system employing short constraint length convolutional codes and Viterbi maximum likelihood decoding on representative fading channels.

Two distinct fading models are considered under both slow and time-varying channel conditions. In the first case, the channel is modeled as a linear combination of a specular and a diffuse scatter component received in the presence of additive white Gaussian noise (AWGN). Assuming further that the diffuse scatter component can be represented as a complex zero-mean Gaussian process conditional upon knowledge of the transmitted signal we have the classical Rician fading channel [4]. In the second case, the amplitude fluctuations are assumed lognormally distributed while the phase perturbations are modeled as a zero-mean Gaussian process both operating independently in the presence of AWGN. The Rician channel provides an appropriate model for fading situations where the transmitted signal undergoes reflection or surface scattering from a large number of distinct

[1] This work was supported in part by NASA under Contract NGR33-018-188.

independent elements or point scatterers. Examples include: HF ionospheric and/or tropospheric scatter links [5]; the aeronautical channel [6]; orbital dipole belts or chaff clouds [7]. The lognormal channel, on the other hand, provides an appropriate model for fading situations characterized by volume scattering (cf. [8], [9]). Here the transmitted signal undergoes fading as a result of random modulation of the refractive index along the transmission path as might result, for example, from turbulent atmospheric effects at microwave or optical frequencies. Both models have been considered for the planetary entry channel [10]. Fortunately, nearly identical performance is obtained when the parameters of the two models are related by an empirical procedure to be described.

Preliminaries. A block diagram of the pertinent aspects of the MFSK data link under consideration is illustrated in Fig. 1. The encoder output sequence n $\{x_i\}$ is drawn from an M-ary alphabet, i.e., $x_i \epsilon \{0,1,...,M-1\}$ for some $M=2^n$. The encoding scheme considered here has been described previously in [3]. In particular, the information bits are assumed shifted into the encoding register one bit at a time. After each shift n modulo 2 sums are performed on the contents of the K-stage encoding register to produce one M-ary symbol for subsequent transmission over the channel. The normalized rate in information bits per channel use is then unity and the corresponding channel signaling waveform is given by

$$s(t) = \sqrt{\frac{2E_b}{T_s}} \sum_i \cos(\omega_{x_i} t + \phi_i)\, p(t - iT_s) \tag{1}$$

where p(t) represents a unit amplitude pulse wayeform of duration T_s seconds, E_b is the energy per transmitted information bit and

$$\omega_i = \omega_0 + i\,\Delta\,\omega \quad ; \quad i=0,1,\ldots,M-1 \tag{2}$$

is the signaling frequency corresponding to the i'th tone with ω_0 representing the lower bandedge of the transmitted signal spectrum and $\Delta\omega$ the fixed frequency increment between adjacent tones. It will be assumed that $\Delta\omega$ is an integer multiple of $2\pi/T_s$ so that, in particular, the signaling tones are orthogonal. The sequence $\{\phi_i\}$ appearing in (1) is a sequence of independent and identically distributed (i.i.d.) random variables uniformly distributed over $[-\pi,\pi]$. The independence is required due to the assumption of noncoherent reception.

The received signal is assumed of the form

$$r(t) = \tilde{s}(t) + n(t) \tag{3}$$

where n(t) is a zero-mean WGN process with double-sided noise spectral density $N_0/2$ watts/Hz and $\tilde{s}(t)$ represents the signal component appearing at the channel output given by

$$\tilde{s}(t) = \sqrt{\frac{2E_b}{T_s}}\, A(t) \sum_i \cos(\omega_{x_i} t + \phi_i + \theta(t)) p(t - iT_s) \tag{4}$$

Here A(t) and θ(t) are respectively amplitude and phase perturbation processes representing the effects of channel fading. We consider two distinct channel models:

Rician Channel: Here we assume that

$$A(t) = |\Gamma + a(t)| \tag{5a}$$

and

$$\theta(t) = \arg[\Gamma + a(t)] \tag{5b}$$

with $\Gamma = \gamma e^{j\psi}$ a complex quantity whose amplitude γ is fixed and deterministic while the phase is uniformly distributed over $[-\pi, \pi]$. The quantity a(t) is a complex zero-mean wide-sense stationary (w.s.s.) Gaussian random process completely described in terms of a channel scattering function $\tilde{\sigma}(f,\tau)$ as described in [7]. As in previous work [3], [11] we consider channels dispersive only in frequency. In particular, we consider general n^{th} order Butterworth frequency dispersion functions of the form

$$\tilde{\sigma}(f;n) = \frac{n\sigma_a^2 \sin(\pi/2n)}{2\pi} \cdot \frac{B_0^{2n-1}}{B_0^{2n} + f^{2n}} \quad ; \quad n \geq 1 \tag{6}$$

with B_0 the single-sided 3dB bandwidth in Hz. The corresponding single-sided fading bandwidth, or equivalently the doppler spread, is given by

$$B_n = \frac{\int_{-\infty}^{\infty} \tilde{\sigma}(f;n)\, df}{2\tilde{\sigma}(0;n)} = \frac{\pi B_0}{2n \sin(\pi/2n)} \quad ; \quad n \geq 1 \tag{7}$$

At any rate, the resulting autocorrelation function of the a(t) process in (5) is then

$$R_{aa}(\tau) = E\{a(t+\tau)a^*(t)\} = 2\int_{-\infty}^{\infty} \tilde{\sigma}(f;n) e^{j2\pi f} \, df \tag{8}$$

which can be conveniently expressed in normalized form according to

$$\rho_{aa}(\tau) \triangleq R_{aa}(\tau)/\sigma_a^2 = \sin(\pi/2n) \sum_{k=1}^{n} \exp\{-2\pi B_0 |\tau| \sin\tfrac{(2k-1)}{2n}\pi\} \sin[\tfrac{(2k-1)}{2n}\pi + 2\pi B_0 |\tau| \cos\tfrac{(2k-1)}{2n}\pi] \tag{9}$$

The amplitude or envelope process A(t) then possesses the Rician probability density function p.d.f.

$$f(A) = \frac{A}{\sigma^2} \exp\left\{-\frac{A^2+\gamma^2}{2\sigma^2}\right\} I_0\left(\frac{A\gamma}{\sigma^2}\right) \quad ; \quad A \geq 0 \tag{10}$$

where $I_0(\cdot)$ is the modified Bessel function of the first kind of order zero and $\sigma^2 = \sigma_a^2/2$ is the common variance of the inphase and quadrature components of a(t). It will prove convenient to impose the normalization

$$E\{A^2\} = \gamma^2 + \sigma_a^2 = 1 \tag{11}$$

which essentially insures a constant received energy. The ratio $\zeta \triangleq \gamma^2/\sigma_a^2$ then represents the ratio of specular to diffuse energy.

We will assume that the a(t) process varies slowly relative to an elementary signaling interval of duration T_s seconds so that it can be considered constant over any such interval but allowed to vary from interval-to-interval. This is a reasonable assumption for B_0T_s <<1. As a result, the received signal in (4) can be expressed as

$$\tilde{s}(t) = \sqrt{\frac{2E_b}{T_s}} \sum_i A_i \cos(\omega_{x_i} t + \phi_i + \theta_i) p(t - iT_s) \tag{12}$$

where $A_i = |\Gamma + a_i|$, $\theta_i = \arg[\Gamma + a_i]$ and a_i represents the -value of the a(t) process throughout the i^{th} signaling interval. The sequence $\{a_i\}$I can be described by the first-order regression

$$a_i = \rho a_{i-1} + w_i \quad ; \quad i=1,2,... \tag{13}$$

where w_i is an i.i.d. sequence of zero-mean complex Gaussian random variates with common variance $(1-\rho 2)\ \sigma_a^2$ and $\rho = \rho_{aa}(T_s)$, which depends only upon the dimensionless product B_0T_s representing channel memory measured in signaling intervals.

Lognormal Channel: I n this case, the amplitude process is defined according to

$$A(t) = \exp\{\chi(t) + m_\chi\} \tag{14}.$$

where m_χ is a fixed constant and $\chi(t)$ is a zero-mean w.s.s. Gaussian process with variance σ_χ^2. The phase process $\theta(t)$ is likewise assumed a zero-mean Gaussian process independent of $\chi(t)$ and possessing variance σ_θ^2. Both $\chi(t)$ and $\theta(t)$ will be assumed to possess n^{th} order Butterworth spectra with 3dB bandwidths B_χ and B_θ respectively. The corresponding p.d.f. of the envelope process is then given by

$$f(A) = \frac{1}{A\sqrt{2\pi\sigma_\chi^2}} \exp\left\{-\frac{(\ell nA - m_\chi)^2}{2\sigma_\chi^2}\right\} \quad ; \quad A \geq 0 \tag{15}$$

Again we impose the constraint $E\{A^2\} = 1$ which implies, in particular, that $m_\chi = \sigma_\chi^2$.

Assuming relatively slow fading, both A,(t) and $\theta(t)$ can be considered constant throughout a specified signaling interval. The sequences $\{A_i\}$ and $\{\theta_i\}$ appearing in (12) can then be generated recursively as in the Rician case.

Correspondence Between Channel Models: It is highly desirable to develop a correspondence relating the parameters of the two channel models under consideration. A useful empirical correspondence has been developed in[10] by equating first and second moments as well as the r.m.s. bandwidths of the envelope and phase process A(t) and $\theta(t)$ respectively. The mean value $m_A E\{A(t)\}$ of the envelope process for the Rician channel can be shown (cf. [12], Appendix F) to be given by

$$m_A = \frac{1}{2}\sqrt{\frac{\pi}{1+\zeta}} \exp\{-\frac{\zeta}{2}\}[(1+\zeta)I_0(\zeta/2)+I_1(\zeta/2)] \tag{16}$$

with $I_\nu(\cdot)$ the modified Bessel function of the first kind of order ν. In the lognormal case, on the other hand, we have

$$m_A = \exp\{-\frac{\sigma_\chi^2}{2}\} \tag{17}$$

so that equating thest two expressions it is possible to solve for ζ in terms of σ_χ^2. A plot of the relationship between σ_χ^2 and ζ is provided in Fig. 2. Note in particular that corresponding to ζ=10 we find σ_χ^2 =0.045 while the limiting case σ_χ^2 =0.242 corresponds to ζ=0 (Rayleigh channel). Observe also that the relationship $\zeta = 1/2\ \sigma_\chi^2$ provides a good approximation over most of the region illustrated and in particular in the weak fading regime (i e.,σ_χ^2 <<1, ζ>>1).

Similarly, a correspondence between B_0 and $B\chi$ can be developed by equating r.m.s. bandwidths of the envelope process A(t) obtained under the two models with the result

$$B_0 = \sigma_\chi\sqrt{2(1+\zeta)}\left[\frac{\sin(3\pi/2n_a)\sin(\pi/2n_\chi)}{\sin(\pi/2n_a)\sin(3\pi/2n_\chi)}\right]^{1/2} B_\chi \tag{18}$$

where n_a and n_χ are the order of the Butterworth spectra generating a(t) and $\chi(t)$ respectively. The details are provided in [10]. It is implicitly assumed that n_a, n_χ>1 since mean-square bandwidths do not exist otherwise. Nevertheless, even in the case $n_a = n\chi = 1$ we will assume that B_0 and B_χ are related by the limiting form of (18) as n_a, $n_\chi \to 1$ i.e.,

$$B_0 = \sigma_\chi\sqrt{2(1+\zeta)}\ B_\chi \tag{19}$$

Finally, making use of the approximate correspondence $\zeta = 1/2\ \sigma_\chi^2$ valid for weak-to-moderate fading we have $B_0 \approx B_\chi$.

Receiver/Decoder Implementation. During each successive signaling interval the noncoherent MFSK receiver computes the M statistics.

$$z_{mi} = \frac{4}{N_0 T_s}\left\{\int_{(i-1)T_s}^{iT_s} r(t)\cos\omega_m t\,dt\right\}^2 + \frac{4}{N_0 T_s}\left\{\int_{(i-1)T_s}^{iT_s} r(t)\sin\omega_m t\,dt\right\}^2 ; i=1,2,.. \quad (20)$$

for m=0,1,...,M-1. The actual receiver output in this case is the sequence $\{\underline{r}_i\}$ where for each i, $\underline{r}_i$ is an M-vector consisting of the components z_{mi}, m=0,1,...,M-1. This will be referred to as the unquantized case. In practice it is desirable to quantize the receiver outputs in some fashion to facilitate decoding operations. The particular quantization scheme considered here results in an ordered list of the ℓ largest decision statistics computed during successive signaling intervals. More specifically, in this case $\underline{r}_i$ is the ℓ-vector

$$\underline{r}_i = (r_{i1}, r_{i2}, \ldots, r_{i\ell}) \quad ; \quad i=1,2,... \quad (21)$$

where r_{ij}=m mϵ{0,1,...,M-1} provided z_{mi} is the j^{th} largest decision statistic $1\le j\le\ell$ computed during the i^{th} signaling interval. The case ℓ=1 corresponds to the conventional hard decision receiver while if ℓ>1 additional reliability information is passed to the decoder. We refer to this case as list-of-ℓ decoding [13].

The receiver output sequences are decoded by means of the Viterbi algorithm. The decoder is not truly maximum likelihood in the sense that suboptimum. decoding metrics are employed. In particular, the decoding strategy is to announce that code sequence as having been transmitted which maximizes the path metric

$$d(\underline{r},\underline{x}^{(j)}) = \sum (\underline{r}_i, x_i^{(j)}) \quad (22)$$

over all paths $\underline{x}^{(j)}=(x_1^{(j)},x_2^{(j)},...)^i$ j=1,2... given the receiver output sequence $\underline{r}=(\underline{r}_1,\underline{r}_2,...)$. Here $\underline{r}_i$ is the receiver output during the i^{th} signaling interval while $x_i^{(j)}$ represents the corresponding encoder output symbol along the j^{th} path. The branch metric $\rho(\underline{r}_i, x_i^{(j)}$ in (22) computed for the i^{th} symbol along the j^{th} path and is different depending upon whether quantized or unquantized receiver outputs are employed. We consider each of these cases separately.

Unquantized Receiver Outputs: For unquantized receiver outputs the branch metric is computed according to

$$\rho(\underline{r}_i, x_i^{(j)}=m)=z_{mi} \quad ; \quad m=0,1,\ldots,M-1 \quad (23)$$

with z_{mi} given by (20). The resulting linear combining law can be shown [14], [15] to be optimum only for the Rayleigh channel (i.e., Rician Channel with ζ=0). Results in [14]

indicate this choice results in little degradation on the Rician channel for any . Similar conclusions are anticipated on the lognormal channel although this has not yet been verified.

Quantized Receiver Outputs: For a list-of-ℓ decoding, the appropriate branch metrics become

$$\rho(\underline{r}_i, x_i^{(j)}=m)=\begin{cases}\log[Mp_M^{(k)}] & ; \text{ if } r_{ik}=m \text{ for some } 1\le k\le \ell \\ \log[\frac{M}{M-\ell} q_M^{(\ell)}] & ; \text{ if } r_{ik}\neq m \text{ for any } 1\le k\le \ell\end{cases} \tag{24}$$

Here $p_M^{(k)}$ is simply the probability that a given symbol was transmitted and resulted in rank k=1,2,...,M at the receiver output. The quantity $q_M^{(k)}$ in (24) is given by

$$q_M^{(k)} = 1 - \sum_{j=1}^{k} p_M^{(j)} \quad ; \quad k=1,2,..,M \tag{25}$$

i.e., the probability that the assumed transmitted branch symbol resulted in rank greater than k.

Performance with Viterbi Decoding . In determining upper bounds on bit error probability with convolutional encoding and Viterbi decoding it is useful to recall the state diagram and associated generating function approach described in some detail in [10]. Assume that the all-zero message has been transmitted and unquantized receiver outputs are employed. Consider some path which remerges with the correct all-zero message having diverged at some point in the past and differing from the all-zero path in exactly k symbol positions. Define the k-vectors

and
$$\underline{A}_k = (A_{k_1}, A_{k_2}, \ldots, A_{k_k}) \tag{26a}$$
$$\underline{\theta}_k = (\theta_{k_1}, \theta_{k_2}, \ldots, \theta_{k_k}) \tag{26b}$$

where A_{k_i} and θ_{k_i} i=1,2,...,k represent respectively the value of the envelope and phase process throughout the i^{th} signaling interval in which the selected incorrect path differs from the all-zero path. Assuming noncoherent MFSK signaling it can be shown that (cf.[14]) that the conditional probability of the error event of rejecting the correct all-zero path for the first time at some level in favor of this incorrect path is independent of $\underline{\theta}_k$ and depends only upon $\underline{A}_k$ according to

$$P_{E|\underline{A}_k} = \frac{e^{-E/N_0}}{2^k\Gamma(k)} \sum_{j=0}^{k-1} \frac{\Gamma(k+j)}{2^j j!} {}_1F_1(k+j;k;E/2N_0) \tag{27}$$

where $\Gamma(\cdot)$ is the Gamma function, ${}_1F_1(m;n;z)$ is the confluent hypergeometric function [17] and finally

$$E \triangleq E_b \sum_{i=1}^{k} A_{k_i}^2 \tag{28}$$

At this point a union bound approach can be applied to obtain an upper bound on the bit error probability P_b by summing the probability of all error events as described above each weighted by the number of nonzero information bits along the corresponding incorrect path. This information is implicit in the code generating function T(D,N). This is a relatively straightforward application of an approach described in some detail in [16] and applied previously to the evaluation of coded system performance on the Rician channel in [11],[14]. The development here will follow closely that of the latter references. In particular, we consider separately the two cases of slow and time-varying fading. Slow fading implies the fading amplitude is constant throughout an entire message sequence, or infinite channel memory, while in the case of time-varying fading the fading amplitude is assumed independent in successive signaling intervals. As a result, the sequence $\{A_i\}$ of fading amplitudes is i.i.d. and represents the opposite extreme of zero channel memory. This can be achieved with suitably large interleaving as argued previously in [11], [14].

Slow Fading Channel: Here we assume $A_{k_i}=A$ i=1,2,...,k where A is a random variable possessing either the Rician p.d.f. given by (10) or the lognormal p.d.f. as described by (15). In principle it is possible to apply the union bound procedure to obtain a bound on the conditional bit error probability $P_{b.A.}$ which can then be averaged over A to obtain a bound on the unconditional bit error probability P_b. Unfortunately, the bound has been found to be tight only for weak fading conditions (i.e., $\zeta>>1$, $\sigma_\chi^2<<1$). As a result we adopt the approach described previously in [11], [14] of utilizing carefully compiled simulation results obtained on the AWGN channel to predict performance on the slow fading Rician or lognormal channel. More specifically, suppose that the simulated performance for a selected code in AWGN is given by $P_b' = g(E_bN_o)$-a numerically tabulated function. Then the predicted bit error probability performance on the slow fading channel is obtained according to

$$P_b = \int_0^\infty g(E_bA^2/N_0)f(A)\,dA \tag{29}$$

with f(A) given by either (10) or (15) for the Rician and lognormal channels respectively. Typical results are illustrated in Fig. 3 for the Rician channel and in Fig. 4 for the lognormal channel where a K=6, M=8 code[2] has been employed in each case. Note that on

[2] Here and throughout the remainder of this paper we shall employ exclusively the optimum M-ary codes as tabulated in [14].

the slow fading channel, the correspondence developed previously is of little value in predicting performance between the two channel models except for extremely weak fading. This behavior is entirely to be expected since, although constrained to have identical first and second moments, the two distributions differ considerably except in the weak fading regime.

Time Varying Channel: It is shown in [14] that under the assumed independence of the components of $\underline{A}_k$ a useful bound on the conditional error event probability in (27) is given by

$$P_{E|\underline{A}_k} \leq \left(\frac{e}{4}\right)^{k/2} \exp\{-\frac{E}{4N_0}\} \{1+0[(E/2N_0)^{-1}]\} \tag{30}$$

Neglecting higher order terms in $(E/2N_0)^{-1}$ and averaging with respect to the components of $\underline{A}_k$ we obtain the following bound on the unconditional error event probability

$$P_E \leq \left(\frac{e}{4}\right)^{k/2} E\left\{\exp\left\{-\frac{E_b}{4N_0}\sum_{i=1}^{k} A_{k_i}^2\right\}\right\} = \left(\frac{e}{4}\right)^{k/2} E^k\left\{\exp\left\{-\frac{E_b A^2}{4N_0}\right\}\right\} \tag{31}$$

where $E\{\cdot\}$ is the expectation operator, A is a generic variate possessing either Rician or lognormal distribution and we have made use of the i.i.d. assumption in stating this last equality. In [14] it is shown that if A is Rician then

$$E\left\{\exp\left\{-\frac{E_b A^2}{4N_0}\right\}\right\} = \frac{1}{1+\frac{E_b}{4N_0(1+\zeta)}} \exp\left\{-\frac{\frac{\zeta}{1+\zeta}(E_b/4N_0)}{1+\frac{E_b}{4N_0(1+\zeta)}}\right\} \tag{32}$$

It follows by applying the union bound procedure that in this case

$$P_b \leq \left.\frac{dT(D,N)}{dN}\right|_{N=1,D=D_0} \tag{33}$$

where

$$D_0 \triangleq \frac{\sqrt{e}}{2\left(1+\frac{E_b}{4N_0(1+\zeta)}\right)} \exp\left\{-\frac{\frac{\zeta}{1+\zeta}\frac{E_b}{4N_0}}{1+\frac{E_b}{4N_0(1+\zeta)}}\right\} \tag{34}$$

This bound is readily evaluated as a function of E_b/N_0 and ζ for selected short constraint length codes and represents the ultimate performance that can be obtained with sufficiently large interleaving. In Fig. 5 we illustrate typical results for 16-ary signaling alphabets all with ζ=10dB. Additional numerical results can be found in [11].

For the time-varying lognormal channel it is easily shown that (33) continues to hold where now

$$D_0 = \int_0^\infty \exp\left\{-\frac{E_b A^2}{4N_0}\right\} f(A)\, dA \tag{35}$$

with f(A) the lognormal p.d.f. given by (15). Unfortunately a closed form expression has not been found for the right-hand side similar to (33) for the Rician channel. Nevertheless, the upper bound can be evaluated by numerical techniques for selected values of E_b/N_o and σ_χ^2. Typical results for 8-ary signaling are illustrated in Fig. 6 for σ_χ^2 =0.045 where the corresponding results for the Rician channel with ζ=10 are also provided. Observe that the results compare favorably with the corresponding Rician channel results. The conclusion to be drawn is that nearly identical performance is to be expected provided the parameters of the two channel models are related under the correspondence developed previously. This is in sharp distinction to the results observed for the slow fading channel where performance was a sensitive function of the amplitude probability distribution.

Simulation Results. Extensive simulation results have been obtained to support and/or extend the analytical results of the preceding section. Of particular interest have been the effects of channel memory and receiver quantization. We will attempt to summarize these findings here.

Effects of Channel Memory: Of interest here is the bit error probability performance parameterized by the fading bandwidth, or equivalently the doppler spread, normalized to the signaling rate $f_s=1/T_s$ Hz. The approach is to provide simulation results only for first order Butterworth fading spectra in either the Rician or lognormal case. In the former case, performance is then conveniently parameterized in terms of the dimensionless quantity B_0T_s. Performance for higher order fading spectra is easily inferred from a comparison of the corresponding normalized autocorrelation given in general by (9). Similarly, for the lognormal channel we will assume a first order Butterworth spectra for the logamplitude process $\chi(t)$. Rather than parameterize performance in this case by $B_\chi T_s$ we have chosen instead to continue the parameterization in terms of B_0T_s.

This latter quantity now represents the B_0T_s value of a fictitcious Rician channel obtained under the correspondence developed previously. In particular, B_0T_s is related to the corresponding value of $B_\chi T_s$ through (18) and the sequel. This parameterization has the advantage of allowing comparison of Rician and lognormal results on a normalized scale.

Typical results for noncoherent MFSK employing unquantized receiver, outputs is illustrated in Fig.'s 7 and 8 for a Rician (ζ=10) and lognormal (σ_χ^2 =0.045) channel respectively. A K=6, M=8 code has been employed in either case. Note that the analytical

performance results of the preceding section provide fairly accurate predictions of actual system performance in the two extremes of zero and infinite channel memory. Observe that in either case for B_0T_s <0.1 there is rapid degradation in performance while, for B_0T_s =0.1 there is little difference from the limiting zero-memory case. This behavior has been observed for a wide range of codes and/or channel parameters. Previous comments (cf. [11], [14]) concerning interleaver requirements apply here. In particular, enough interleaving should be provided to result in an[3] "effective" B_0T_s in the vicinity of 0.1.

Receiver Quantization Effects: Typical results for noncoherent MFSK evploying list-of-ℓ receiver quantization is illustrated in Fig. 9 for a Rician channel with ζ=10. Here using a full list decoding metric approximately 0.6 dB degradation is incurred vis-à-vis infinitely fine quantization. For the AWGN channel this degradation is only a few tenths of a dB while under more severe fading this degradation can amount to as much as 2.5 dB on the Rayleigh channel. Similar comments apply in the case of lognormal fading. As a result, alternatives to the list-of-ℓ quantization scheme should be employed under severe fading conditions.

Summary and Conclusions. A Detailed analysis has been presented of the performance of short constraint length convolutional codes in conjunction with noncoherent MFSK modulation on fading channels. Both the classical Rician fading channel and the lognormal fading channel have been considered. The intent has been to demonstrate useful analytical techniques for predicting the resulting bit error probability performance as a function of code and/or channel parameters as well as receiver implementation. The analytical results have been supported where possible by digital computer simulations. An important conclusion is that coded system can be made relatively insensitive to the choice of channel model provided the parameters are related by an explicit correspondence developed as part of this paper. It is hoped that this work will prove useful to communication systems analysts concerned with the evaluation of coded system performance in fading channel environments.

References

1. A.J.Viterbi and I.M.Jacobs, "Advances in Coding and Modulation for Noncoherent Channels Affected by Fading, Partial Band, and Multiple-Access Interference", Chap 7 in Advances in Communication Systems, Vol. 4, Ed. by A.J.Viterbi, Academic Press, New York, 1975.

2. D. Chase, "Digital Signal Design Concepts for a Time-Varying Rician Channel", IEEE Trans. Commun. Vol. COM-24, No. 2, Feb. 1976, pp.164-173.

[3] In general a block interleaver of size IxL results in an "effective" time-bandwidth product B_0T_s x I.

3. J.W.Modestino and S.Y.Mui, “Performance of Coded MFSK in a Rician Fading Channel”, Proc. of 1975 International Telemetry Conference (ITC) Washington, D.C., Oct. 1975, PP. 178-188.

4. J.M.Wozencraft and I.M.Jacobs Principles of Communication Engineering, John Wiley and Sons, New York, 1965.

5. M. Schwartz, W.R.Bennett and S.Stein. Communication Systems and Techniques McGraw-Hill Book Co., Inc., New York, 1966, Chap. 9.

6. P.A.Bello, “Aeronautical Channel Characterization”, IEEE Trans.Commun. Technol., Vol. COM-21, No. 5, May 1973, Pp. 548-563.

7. R.S.Kennedy, Fading Dispersive Communication Channels, Wiley-Interscience, New York, 1969, Chap. 2.

8. J.Strohbehn, “Line of Sight Wave Propagation Through The Turbulent Atmosphere”, Proc. IEEE, Vol. 56, No. 8, Aug. 1968, pp. 1301-1318.

9. R.L.Fante, “Electromagnetic Bean Propagation in Turbulent Media”, Proc. IEEE, Vol. 63, No. 12, Dec. 1975, PP. 1669-1692.

10. J.W.Modestino and S.Y.Mui, “Selected Modulation Approaches in Conjunction with Convolutional Encoding on Fading,Channels”, unpublished R.P.I. report.

11. J.W.Modestino and S.Y.Mui, “Convolutional Code Performance in the Rician Fading Channel”, to be published in IEEE Trans. on Communications.

12. C. W. Helstrom, Statistical Theory of Signal Detection, 2nd Ed.,Pergamon Press, New York, 1968.

13. K.L.Jordan, Jr., “The Performance of Sequential Decoding in Conjunction with Efficient Modulation”, IEEE Trans. Commun, Technol., Vol. COM-14, No. 3, June 1966, pp. 283-297.

14. J.W.Modestino and W.Y.Mui, “Noncoherent MFSK in Conjunction with Convolutional Encoding on the Rician Channel”, submitted to IEEE Trans. on Communications.

15. I.M.Jacobs, “Probability-of-Error Bounds for Binary Transmission on the Slowly Fading Rician Channel”, IEEE Trans. Inform. Theory, Vol. IT-12, oct. 1966, pp. 431-441.

16. A.J.Viterbi, “Convolutional Codes and Their Performance in Communication Systems”, IEEE Trans. Commun. Technol., Vol.COM-19, No-5, Oct. 1971, pp 750-772.

17. M. Abramowitz and I.A.Stegun, Ed.’s Handbook of Mathematical Functions, National Bureau of Standards, Applied Math. Series 55.

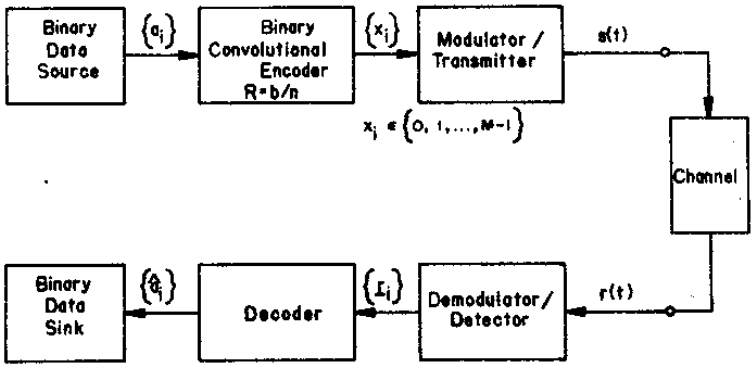

Figure 1 MFSK System Employing Binary Convolutional Coding

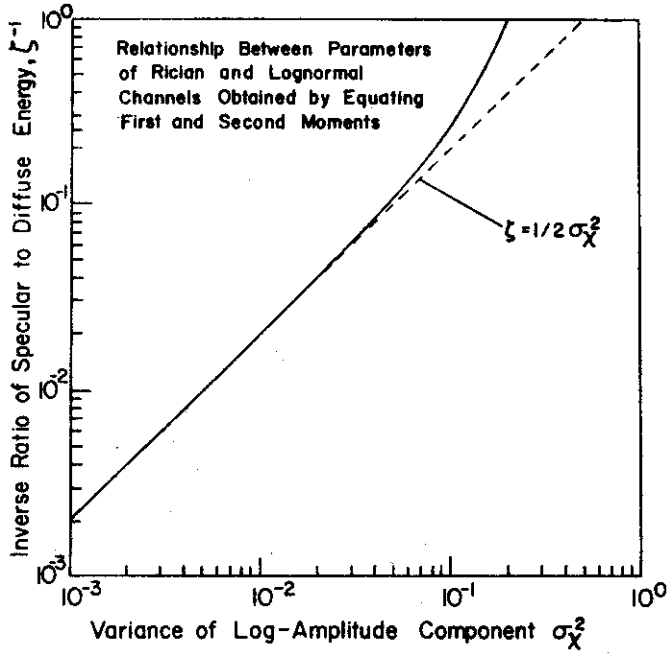

Figure 2 Relationship Between Parameters of Rician and Lognormal Channel

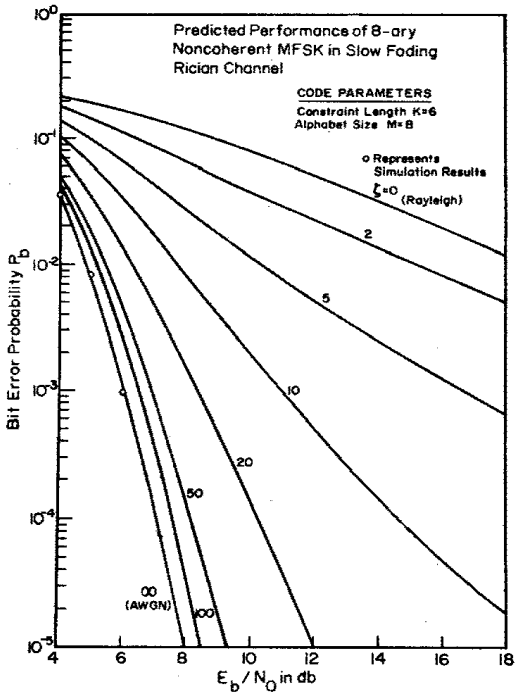

Figure 3
Predicted Performance of 8-ary Noncoherent MFSK on Slow Fading Rician Channel Using K=6 Code

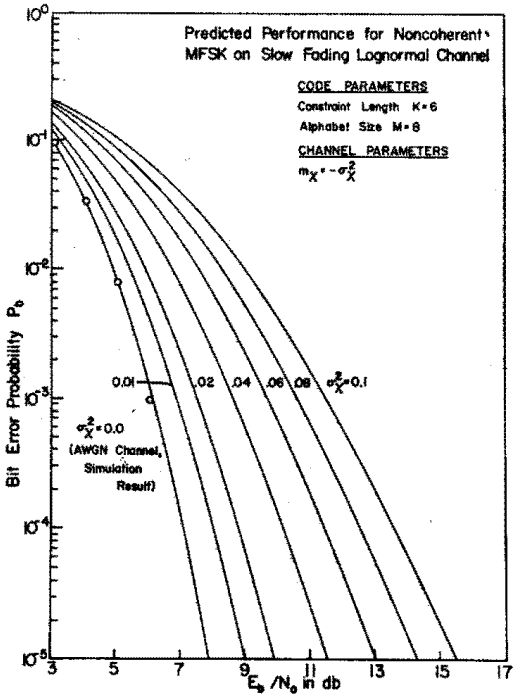

Figure 4
Predicted Performance of 8-ary Noncoherent MFSK on Slow Fading Lognormal Channel Using K=6 Code

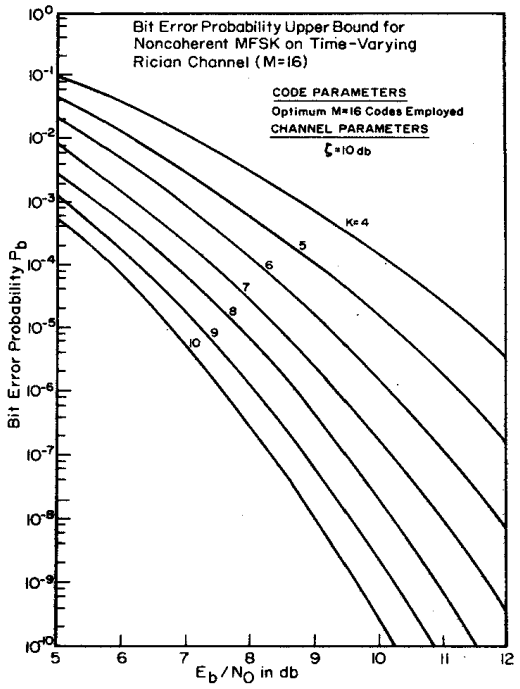

Figure 5
Computed Bit Error Probability Upper Bounds for Noncoherent MFSK Using Selected 8-ary Codes on Time-Varying Rician Channel with ζ=lOdB.

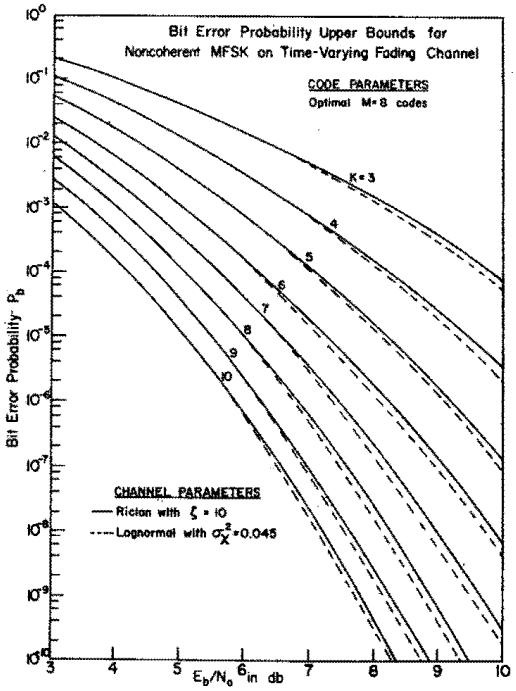

Figure 6
A Comparison of Bit Error Probability Upper Bounds for Noncoherent 8-ary MFSK Operating on Time-Varying Rician and Lognormal Channels

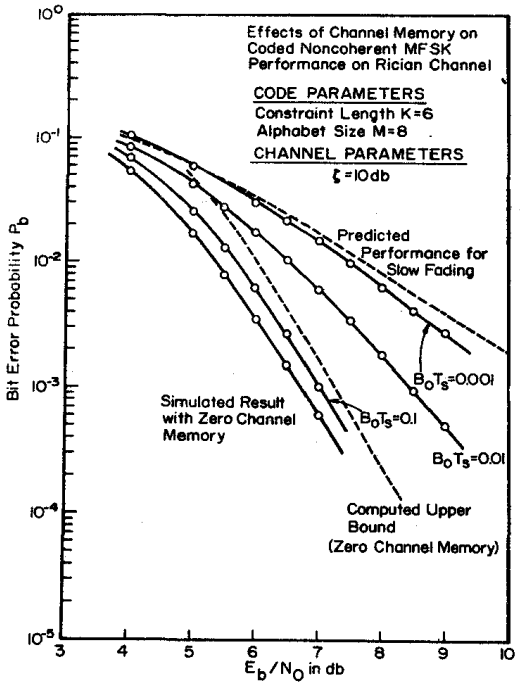

Figure 7
Simulated Performance of Noncoherent 8-ary MFSK Employing K=6 Code on Time-Varying Rician Channel with ζ=10dB

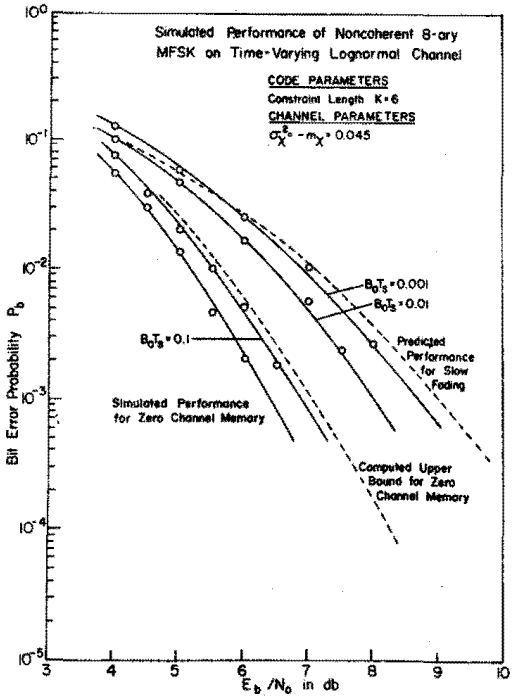

Figure 8
Simulated Performance of Noncoherent 8-ary MFSK Employing K=6 Code on Time-Varying Lognormal Channel with σ^2_χ = 0.045

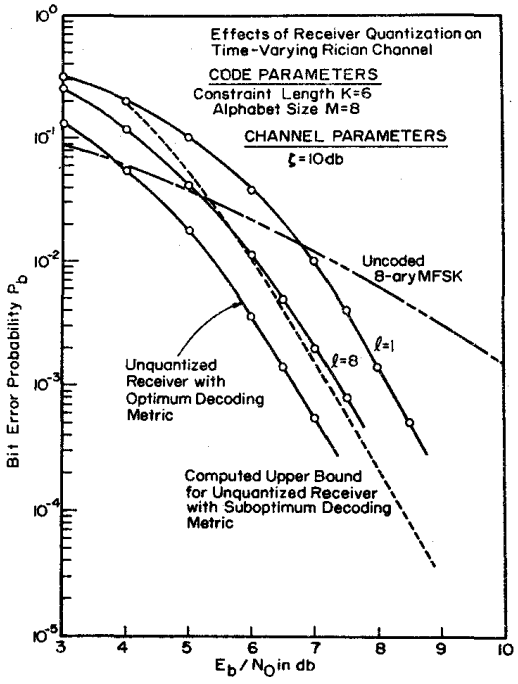

Figure 9
Effects of Receiver Quantization on Noncoherent 8-ary MFSK Performance Using K=6 Code on Time-Varying Rician Channel. Ratio of Specular to Diffuse Energy ζ=10dB.